Anal. Chem. **1998,** *70,* 2881−2887

Viscoelastic Behavior of Antibody Films on a Shear Horizontal Acoustic Surface Wave Sensor

M. Weiss,[†] W. Welsch,[‡] M. v. Schickfus,* and S. Hunklinger

Institut für Angewandte Physik der Universität Heidelberg, Albert-Ueberle-Strasse 3-5, 69120 Heidelberg, Germany

To study the viscoelastic behavior of antibody films on a surface acoustic wave device, we have measured the influence of multiple layers of antibodies onto the propagation of the wave. Attenuation and sound velocity variation caused by up to 20 layers have been measured. The results can be interpreted with the propagation of a viscously damped Love wave in a film with an extremely low velocity of sound. From our results, we conclude that, for the one- or two-layer films normally used in acoustic wave immunosensing, a pure mass effect is dominant. For thick films, a saturation of the sensor response is observed.

Acoustic surface waves (SAWs) are very sensitive to mass changes in their propagation path and, therefore, are an interesting tool for mass-sensitive sensors.[1] Recently, this technique has been applied to immunosensing, and detection limits of the order of 33 pg for a sensor area of 5 mm^2 have been achieved.[2]

In an immunosensor application, a SAW delay line is covered by a sensitive film, usually consisting of immobilized antibodies, which are capable of selectively binding the antigen to be detected. The increase of mass associated with the binding leads to a variation of the SAW velocity which can be detected by a change of phase of the output signal of the delay line. For experimental purposes, the antigens to be detected are antibodies as well. They possess amino groups fitting the antigen binding sites of the previously immobilized sensitive antibody film.

SAW immunosensors operate in liquids (normally buffer solutions). Apart from technical problems associated with isolating the SAW device electrically and chemically from the liquid,[3] the question arises of how a viscoelastic film consisting of antibodies bound to each other and to the SAW device surface behaves when coupled to an acoustic wave at a frequency of a few hundred megahertz.

Immobilized antibodies such as the ones used in our investigations form layers about 10 nm thick. Until now, their acoustic behavior, i.e., their elastic and viscous properties, were essentially neglected. For an interpretation of the results, only a mass increase was considered. Many questions, however, remained unanswered. Is the antibody film a dense layer of protein, or is it filled with water like a sponge? What are the elastic constants and the viscosity of this film? And to what thickness does the acoustic wave penetrate into this film?

Information about these properties is necessary for an optimization of the sensitivity of such sensors and for a quantitative interpretation of the results obtained.

THEORY

A surface acoustic wave (SAW) propagating in the x_1 direction on a substrate can be described by

$$u_j(x, t) = U_j(x_3)\, \epsilon^{i(\gamma x_1 - \omega t)} \qquad (j = 1, 2, 3) \tag{1}$$

where γ denotes the complex propagation factor of the wave, which reduces to the wave vector k_0 in the lossless case, and $\omega = 2\pi f$ is the angular frequency. U_j contains information about the type of the wave (polarization, etc.). In most cases, it is a function decreasing exponentially with x_3, reflecting the finite penetration depth of the surface wave into the substrate.

External influences on such a wave (e.g., variation of the elastic coefficients of the surface by coating the substrate) give rise to a perturbation of the propagation factor. The normalized perturbation of γ can be written as[4]

$$\frac{\Delta\gamma}{k_0} = \frac{\Delta\alpha}{k_0} - i\frac{\Delta v}{v_0} \tag{2}$$

Here, $\Delta\alpha/k_0$ denotes the attenuation per wavenumber and $\Delta v/v_0$ the relative change of the wave velocity.

Coating the surface with a viscoelastic film of thickness h will, therefore, change the wave velocity very specifically and may also cause losses. In Figure 1, the typical setup of a partly coated substrate with a propagating SAW is shown.

Characterization of Viscoelastic Films. In the following sections, the perturbation caused by coating a SAW device with a thin isotropic viscoelastic layer is of special interest; therefore, some characteristics of such layers will be summarized.

[†] MPI für Strömungsforschung, Abteilung für Nichtlineare Dynamik, Bunsenstr. 13, D-37073 Göttingen, Germany.

[‡] Robert Bosch GmbH, Geschäftsbereich K1 Entwicklung Weg/Winkelsensoren, Postf. 300240, D-70442 Stuttgart, Germany.

(1) Grate, J. W.; Martin, S. J.; White, R. M. *Anal. Chem.* **1993**, *65*, 940−948; 987−996.

(2) Welsch, W.; Klein, C.; Schickfus, M. v.; Hunklinger, S. *Anal. Chem.* **1996**, *68*, 2000−2004.

(3) Schickfus, M. v.; Welsch, W.; Weiss, M.; Hunklinger. S. *Proceedings of the 1997 IEEE Frequency Control Symposium*, Orlando, FL, 1997.

(4) Auld, B. A. *Acoustic Fields and Waves in Solids*; Robert Krieger Publishing Co.: Malabar, FL, 1990.

S0003-2700(97)01006-8 CCC: $15.00
Published on Web 06/12/1998

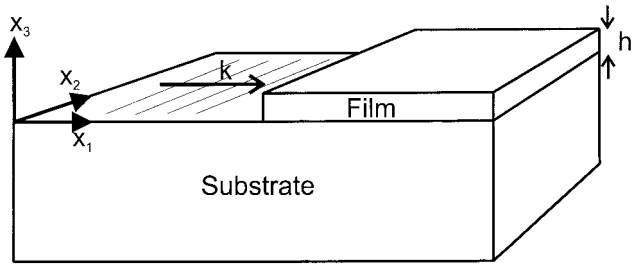

Figure 1. A device partly coated with a film of thickness *h*. The coordinate system used in this work and the direction of wave propagation are also shown; the SAW wave fronts are sketched by parallel lines perpendicular to the wave vector *k*.

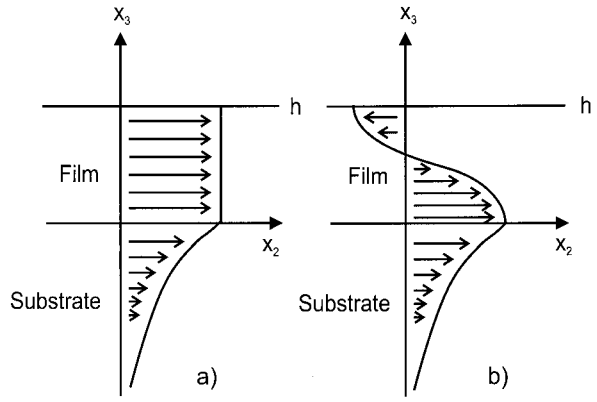

Figure 2. Schematic representation of an acoustically thin and an acoustically thick film. A shear horizontal SAW with an exponentially decreasing amplitude in the substrate with two different types of coating is shown. In an acoustically thin film (a), the film is displaced in a constant continuation of the displacement at the substrate surface. In an acoustically thick film (b), the displacement profile varies throughout the film, so that upper and lower boundary planes may move with a relative phase of 180°.

Both elastic coefficients of isotropic viscoelastic materials are complex quantities,[5] where the real part describes the elastic storage modulus and the imaginary part the dissipative loss modulus: $G = G' + iG''$ (shear modulus), $K = K' + iK''$ (bulk modulus). Thus, an ideal elastic film would have $G'' = K'' = 0$. Harmonic excitation of viscoelastic media with angular frequency ω leads to $G'' = \eta\omega$, where η denotes the dynamic viscosity.

For simplicity, we will limit the following discussion to shear horizontal excitation; the concept, however, can easily be expanded to any type of wave.

In the case of shear excitation, the behavior of an isotropic film on the surface of a SAW device will depend on its shear modulus G and its thickness h. If it is *acoustically thin*, it will follow the SAW excursion at the substrate surface with negligible internal strain (Figure 2a). In the *acoustically thick* case, however, the film will be strained (Figure 2b). A quantity describing the acoustic behavior of a thin viscoelastic film must, therefore, include the ratio $\omega/|G|$ and the thickness h of the film. Such a measure for very thin films ($hk_0 \ll 1$) has been defined by Martin et al.:[7]

$$R = A\rho v_0 \frac{\omega h}{|G|} \approx hk_0 \frac{{v_0}^2}{{v_F}^2} \qquad (3)$$

Here, v_0 and k_0 are the SAW velocity and the wave vector in the substrate, respectively, and v_F is the shear velocity in the film. The factor A, given by

$$A = \frac{2\pi\sqrt{c_2 + c_1}}{\sqrt{c_2 + c_3} + 2\sqrt{c_1}} \qquad \text{with} \qquad c_j = \frac{{\dot{u}_{j0}}^2}{4k_0 P}$$

is a substrate-specific quantity of magnitude 1, which includes the particle velocity components $\dot{u}_{0j}$ at the surface as well as the power density P of the wave.

With $\rho/|G| = v_F$ and $\omega = k_0 v_0$, the approximate expression for R on the right side of eq 3 is obtained. For $R \ll 1$, the film is acoustically thin; for $R \geq 1$, it is acoustically thick, and a Love-type wave can be excited, provided that $v_F < v_0$.[6]

Perturbation Caused by Viscoelastic Films. In the following, an expression for the perturbation of γ derived by Martin et al.[7] will be discussed and applied to our experimental situation. The normalized perturbation of the propagation factor for a SAW device, coated with a thin isotropic viscoelastic layer ($k_0 h \ll 1$) assumed to be acoustically thick, is given by[7]

$$\frac{\Delta\gamma}{k_0} = \sum_{j=1}^{3} \frac{{\dot{u}_{j0}}^2}{4k_0 P} \sqrt{M^{(j)}} \sqrt{\rho - \frac{E^{(j)}}{{v_0}^2}} \tanh\left(\frac{i\omega h}{\sqrt{M^{(j)}}} \sqrt{\rho - \frac{E^{(j)}}{{v_0}^2}} \right) \qquad (4)$$

with

$\dot{u}_j^0$ = particle velocity at the substrate surface

P = power density of the wave

ρ = density of the viscoelastic film

$M^{(j)}, E^{(j)}$ = elastic coefficients of the film

v_0 = phase velocity in the substrate

h = thickness of the viscoelastic film

ω = angular frequency of the wave

As the elastic coefficients $M^{(j)}$ and $E^{(j)}$ play a crucial role here, they are introduced in Appendix A. In brief, they are closely related to the shear and bulk moduli of the film; therefore, only two independent elastic coefficients exist.

For the following calculations, other than in ref 7, only the $j = 2$ component will be regarded.[8] Two special cases of the perturbation formula (eq 4) are of special interest:

(5) Ferry, J. D. *Viscoelastic Properties of Polymers*; Wiley & Sons: New York, 1961.

(6) Farnell, G. W. Types and Properties of Surface Waves. In *Acoustic surface waves*; Oliner, A. A., Ed.; Topics in Applied Physics 24; Springer: Heidelberg, Germany, 1978.

(7) Martin, S. J.; Frye, G. C.; Senturia, S. D. *Anal. Chem.* **1994**, *66*, 2201–2219.

(8) Martin et al. derived their formulas for an acoustic thick polymer coating on a SAW device operating with Rayleigh waves, whereas our devices operate with shear horizontal waves.

(1) Ideal Elastic Film. In this case, the constants $E^{(2)}$ and $M^{(2)}$ are equal to the real Lamé constant μ. Furthermore, for typical film characteristics ($R \ll 1$), the hyperbolic tangent can be replaced by its argument. After separation into real and imaginary parts, the resulting perturbation formula reads

$$\frac{\Delta\nu}{\nu_0} = -\frac{\nu_0 h}{4P}\left(\rho - \frac{\mu}{\nu_0^2}\right)\dot{u}_{20}^2 \qquad \text{and} \qquad \frac{\Delta\alpha}{k_0} = 0 \qquad (5)$$

These are exactly the perturbation formulas for a shear wave device coated with a thin, elastic, lossless film derived in ref 4, which can be used for measuring the mass loading of a SAW device.[2]

(2) Highly Viscous Film. For a highly viscous film, $M^{(2)} \rightarrow i\eta\omega$ is valid, and for typical values the argument in eq 4 is large enough to assume $\tanh(x) \approx 1$. With $E^{(2)} = \rho v_F^2$ and $v_F \ll v_0$ for typical viscous materials, we have $[(\rho - E^{(2)})/v_0^2]^{1/2} \approx \rho^{1/2}$, and with $i^{1/2} = (1 + i)/2^{1/2}$, one finds the following real and imaginary parts:

$$\frac{\Delta\nu}{\nu_0} = -\frac{\dot{u}_{20}^2}{4Pk_0}\sqrt{\frac{\omega\rho\eta}{2}} \qquad \text{and} \qquad \frac{\Delta\alpha}{k_0} = \frac{\dot{u}_{20}^2}{4Pk_0}\sqrt{\frac{\omega\rho\eta}{2}} \qquad (6)$$

These are exactly the perturbation formulas in ref 9 for viscous coating of a shear SAW device.

For arbitrary viscoelastic films, it is no problem to separate the $j = 2$ component of eq 4 into real and imaginary parts. With $(M^{(2)})^{1/2} = m^{(2)\prime} + im^{(2)\prime\prime}$ and $\zeta = [(\rho - E^{(2)})/v_0^2]^{1/2}$, one obtains

$$\frac{\Delta\alpha}{k_0} = \frac{\dot{u}_{20}^2}{4Pk_0}\zeta\,\frac{m^{(2)\prime}\sinh\left(2h\omega\zeta\dfrac{m^{(2)\prime\prime}}{|\sqrt{M^{(2)}}|}\right) - m^{(2)\prime\prime}\sin\left(2h\omega\zeta\dfrac{m^{(2)\prime}}{|\sqrt{M^{(2)}}|}\right)}{\cosh\left(2h\omega\zeta\dfrac{m^{(2)\prime\prime}}{|\sqrt{M^{(2)}}|}\right) + \cos\left(2h\omega\zeta\dfrac{m^{(2)\prime}}{|\sqrt{M^{(2)}}|}\right)} \qquad (7a)$$

$$\frac{\Delta\nu}{\nu_0} = -\frac{\dot{u}_{20}^2}{4Pk_0}\zeta\,\frac{m^{(2)\prime\prime}\sinh\left(2h\omega\zeta\dfrac{m^{(2)\prime\prime}}{|\sqrt{M^{(2)}}|}\right) - m^{(2)\prime}\sin\left(2h\omega\zeta\dfrac{m^{(2)\prime}}{|\sqrt{M^{(2)}}|}\right)}{\cosh\left(2h\omega\zeta\dfrac{m^{(2)\prime\prime}}{|\sqrt{M^{(2)}}|}\right) + \cos\left(2h\omega\zeta\dfrac{m^{(2)\prime}}{|\sqrt{M^{(2)}}|}\right)} \qquad (7b)$$

These perturbation formulas, describing the reaction of a shear horizontal SAW to viscoelastic loading, will be compared with our experimental data.

EXPERIMENTAL SECTION

SAW Devices. The SAW devices used for all measurements were delay lines on a 36° *YX* $LiTaO_3$ substrate with Cr/Au (20/80 nm) interdigital transducers (IDTs) separated by a path length of 4 mm. The delay path between the IDTs was metalized with a thin Cr/Au (20/80 nm) layer. The chosen crystal cut supports a shear horizontal leaky surface wave which propagates nearly undamped.[10] Besides the shear displacement, there is also a vertical component, which will be neglected here, because it is suppressed by a factor of 14.3.[11] The good agreement of the perturbation formulas (eq 7) with our experimental results shows that it is reasonable to do so. The IDTs consisted of 25 splitfinger pairs with a periodicity of 9 μm, for a center frequency of 115 MHz. The IDT pads were gold wire bonded to a commercial chip socket. To protect IDTs and bonding wires from conducting liquids, these sensitive areas were coated with a silicone layer (Dow Corning RTV coating 3140). Only on 3.5 mm of the path length, an uncoated gold surface remained. On every chip there were two of these delay lines. In Figure 3, a typical SAW device is shown.

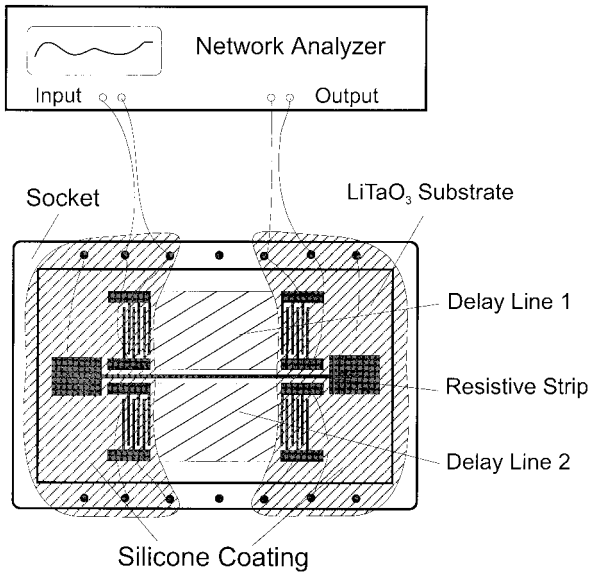

Figure 3. SAW device used in our experiments. Two delay lines are separated by a thin metal strip used for thermometry, the IDTs are coated by silicone. The analyte droplet is in contact only with the gold-covered space between the transducers. All metalization is 80 nm of gold on 20 nm of chromium. Connection with the network analyzer is schematically indicated.

Electronic Instrumentation and Measuring Technique. The measuring temperature was kept close to room temperature by mounting the device onto a brass base plate through which water from a thermostat was circulated. Temperature fluctuations could be monitored by measuring the resistance of a metal strip on the SAW device. In all measurements, temperature was constant within ±0.05 °C.

For our measurements, we used a HP 8752A network analyzer (NA), the output of which was connected to one of the IDTs of the SAW device. The signal received by the opposite IDT after a delay time $\tau = l/v_0$ was fed into the input of the NA. The NA measures phase ϕ and total attenuation L_{dB} of the received signal

(9) Kondoh, J.; Shiokawa, S. *Electron. Commun. Jpn.* **1993**, *76* (2), 69−81.

(10) Yamanouchi, K.; Takeuchi, M. *1990 IEEE Ultrasonic Symposium*; IEEE Publications: New York, 1990; pp 11−18. The attenuation per wavelength for the chosen crystal cut is $\alpha \leq 0.01$ dB/λ.

(11) Nomura, T.; Yasuda, T. *1990 IEEE Ultrasonic Symposium*; IEEE Publications: New York, 1990; pp 307−310.

relative to its output signal. Both quantities were read out and stored in a personal computer, which also controlled the NA to alternately perform measurements at the fundamental frequency of the device (115 MHz) and at the third harmonic (345 MHz). An rf switch allowed for measurements on both delay lines of the device in the same experimental run. Details of the setup can be found in ref 2.

An attenuation change $\Delta\alpha$ caused by the film on the device is related to the output of the network analyzer by $\Delta L_{dB} = 20 \lg(e)\, l_S \Delta\alpha$, where l_S denotes the length of the path between the IDTs exposed to the analyte, from now on referred to as the *sensitive path*.

A phase change of the output signal is related via the frequency−phase relation to the fractional velocity shift by $\Delta\phi = \Delta\omega l/v_0 - \omega l_S \Delta v/v_0^2 = -(l_S/l)(\Delta v/v_0)$, since the NA operates at fixed frequency. Therefore, all perturbation formulas can be expressed in terms of measured quantities $\Delta\phi$ (in degrees) and ΔL_{dB} as

$$\Delta\phi = l_S k_0 \frac{360°}{2\pi}\left(-\frac{\Delta v}{v_0}\right), \qquad \Delta L_{dB} = 20 \lg(e) l_S k_0 \left(\frac{\Delta\alpha}{k_0}\right) \quad (8)$$

The quantities in parentheses represent the perturbation formulas derived in the Theory section.

Biological Preparation. As described by Welsch et al.,[2] antibodies can be detected by a SAW device very easily via the mass effect, because they are rather heavy (molecular weight about 150 000) and have a very specific binding site for matching antigens.

For all measurements, immunoglobulins of type G (IgG) were used. They have a Y-shaped form set up by two light and two heavy chains connected by disulfide bridges. The stem of the IgG is called the crystallizable fragment (F_c), and the branches, according to their function, are called the antigen binding fragment (F_{ab}). The very flexible hinge region connects the fragments. The F_c fragment is known to bind extremely well to protein A,[12] which, in turn, is easily adsorbed onto gold surfaces with a high adhesion coefficient.[13] Alternately, IgG molecules can also be immobilized directly on the gold surface using their disulfide bridges and the high flexibility of the hinge region[14] (Figure 4).

The antigen binding sites of the F_{ab} fragment are specialized to link to certain regions of an antigen, the so-called determinants. This noncovalent antigen−antibody interaction is very specific to the shape and consistency of the determinant and involves hydrogen bonds and electrostatic and van der Waals forces.[12] The specific binding energy is, nevertheless, quite strong (about 40 kJ/mol) and typically 10 times greater than pure van der Waals interaction.[15,16] Despite their specifity, it is a well-known fact that antibodies can also bind to structures which are similar to "their" determinants but may be part of a completely different antigen.

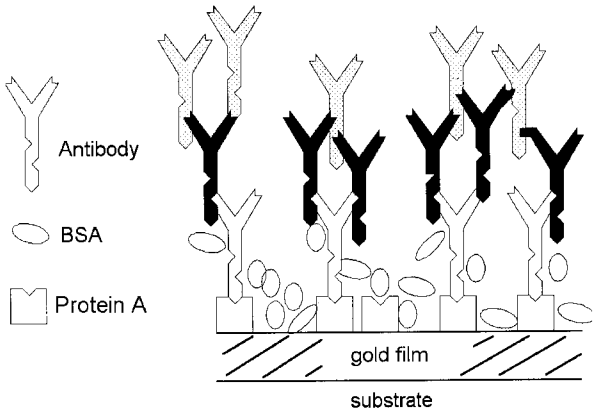

Figure 4. Immobilization of antibodies (open symbols) on a gold surface using the protein A method. A sequence of matching antibodies (black and gray) is bound to the immobilized antibodies. In some of the experiments described later, the protein A was omitted.

These cross reactions are sometimes used in certain precipitation techniques.[17]

In our experiment, we have used so-called polyclonal antibodies, which are sensitive to a distinct antigen but link with their F_{ab} fragment to several determinants. Using a solution of polyclonal antibodies thus enhances the effect of cross reactions.

In our investigation, all antigens to be detected were antibodies themselves, where the F_{ab} fragment of one type of IgG was specific to the F_c fragment of the other. This made it possible to consecutively link several matching antibodies together, resulting in a very soft, spongelike film. We have used three types of matching polyclonal antibodies:[18] (1) AffiniPure rabbit anti-sheep IgG H+L (2.4 mg/mL), (2) AffiniPure sheep anti-mouse IgG H+L (2.4 mg/mL), and (3) AffiniPure mouse anti-rabbit H+L (minimal cross reaction to human, goat, mouse, sheep) (1.9 mg/mL). The devices for all measurements were prepared in the following sequence.[19] The first step is to put a droplet (about 5 μL) of phosphate-buffered saline (PBS) solution onto the sensitive path. With that, the sensor response to the viscosity change from an open sensor to one covered with water is established and serves as a reference for all subsequent measurements.

In the next step, about 5 μL of concentrated antibody solution, e.g., IgG (1) from the above list, is added to this droplet. This causes a second sensor reaction, reflecting the nonspecific adsorption of the biomolecules onto the gold surface (in first order, the SAW will see a pure mass loading[2]). After some time, there is no further adsorption, and the droplet is washed away by rinsing the sensitive path with PBS solution. In this step, due to the strong protein binding, only unbound antibodies are removed.

Then, after putting on a new PBS droplet, a concentrated bovine serum albumin (BSA) solution is added to the PBS droplet instead of antibody solution. BSA saturates all unoccupied gold

(12) Natvig, J. B.; Turner, M. W. The Immunoglobulines. In *Clinical Aspects of Immunology*, 5th ed.; Blackwell Scientific Publications: Boston, MA, 1993.
(13) Yang, M.; Chung, F. L.; Thompson, M. *Anal. Chem.* **1993**, *65*, 3713−3716.
(14) Gosling, J. P. *Methods in Immunological Analysis*, VCH: Weinheim, Germany, 1985.
(15) Krieg, B. *Chemie für Mediziner*; de Gruyter: Berlin, Germany, 1993.
(16) Absolom, D. A.; van Oss, C. *CRC Crit. Rev. Immunol.* **1986**, *6*, 1−46.
(17) Lammers, M.; et al. *Proteindiagnostik*; Behringwerke AG: Frankfurt, Germany, 1991.
(18) DIANOVA Forschungsreagenzien, Immundiagnostik. Produktinformation zu Antikörpern, Hamburg, Germany, 1993.
(19) For the of sake simplicity only the preparation without protein A is described. Using protein A alters the order of preparation in the following way: protein A, BSA, first IgG, second IgG, ...

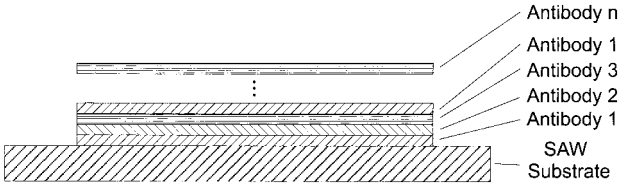

Figure 5. Stacking of a sequence of antibodies. Antibody 2 has specific sites against antibody 1, antibody 3 against antibody 2, and antibody 1 against 3. Using this sequence, stacks of up to 20 antibody sequences have been built.

sites but does not bind to the adsorbed antibodies.[20] After equilibrium is reached, the whole gold surface is coated either by antibodies or by BSA molecules. From then on, only specific binding to the F_{ab} fragment of the immobilized antibody can occur. Like in the previous step, unadsorbed BSA is washed off. All subsequent steps follow this scheme: (a) put a droplet (5 μL) of PBS onto the sensitive path, (b) add 5 μL of a solution of antibodies that match the binding site of the antibodies immobilized at the surface in the previous step, (c) wait until signals are stable again, and (d) wash off the rest of the solution with unbound antigen and then back to (a). With this sequence, it is possible to build a stack of about 20 layers of antibodies, as shown schematically in Figure 5. Additional layers did not yield sensor signals distinguishable from noise. For each step, the change of phase and attenuation associated with increasing the layer thickness from h to h + 10 nm (the thickness of one antibody layer is estimated to be about 10 nm) were measured. A plot of accumulated amplitude and phase shift against total thickness of the film gives information on how the sensor would react if a layer of cross-linked antibodies with this thickness was put onto the naked sensor.

In the procedure described above, the first antigen layer was unspecifically bound to the gold surface. In some of our experiments, we used the protein A method as described in ref 2. The experimental results, however, did not differ with the two preparation methods, except for a slightly higher phase shift after immobilization of the second antibody when using protein A. This effect was probably caused by a better arrangement of the F_{ab} fragments of the first antibody layer on protein A.

RESULTS AND DISCUSSION

If there was no cross reactivity of the antibodies used, the consecutive linkage of them resulted in a formation of long linear chains, where each F_c fragment fits to an F_{ab} fragment of the previously immobilized layer. Thus, no cross-linking and no shear stiffness of the layer should exist; consequently, the whole organic layer always should react acoustically thin, and only mass loading according to eq 5 should be observed. But, as cited above, the cross reactivity leads to a precipitation-like behavior of the molecules; thus, a polymerized antibody layer can form. Due to that, acoustically thick behavior should occur with increasing thickness and the perturbation theory developed above (especially eqs 7a,b) are applicable.

As a first approximation, one would expect the antibody film to have a spongelike structure filled with water, having elastic coefficients similar to those of a very rubbery polymer ($|A| \approx 10^6$ N/m^2) and a density ρ similar to that of water.

In Figure 6, the experimental data for the fundamental frequency (115.3 MHz) and the third harmonic (348 MHz) are shown. Both data sets were measured simultanuosly with the same device and antibody solutions. The full lines represent a simultaneous best fit to eqs 7a and 7b, respectively. As expected, the fitting parameters change slightly with frequency but stay within the same magnitude. From additional measurements, we found all the fits to be characterized by the following values:

$$\rho - \frac{E^{(2)}}{v_0^2} \approx \rho \approx 1000 \text{ kg/m}^3$$

$$Re(M^{(2)}) \approx 10^5 - 10^6 \text{ N/m}^2 \qquad (9)$$

$$\text{Im}(M^{(2)}) \approx 10^6 - 10^7 \text{ N/m}^2$$

These values are very reasonable if compared to the elastic coefficients of very soft polymers, always keeping in mind that the spongelike film is very watery.

Especially case 1 (ideal elastic film) of the theory section is shown to hold until $h \approx 50$ nm for 115 MHz and $h \approx 30$ nm for 348 MHz. This proves that the perturbation formulas for mass loading (eq 5) can, indeed, be used for normal sensor applications, where only about two or three layers of antibodies are used. This agrees well with the results of Welsch et al.[2]

The "saturation tails" in the measurements (Figure 6) display the totally viscous behavior of an antibody film above a certain thickness.[21] For an estimation of the *viscous penetration depth* δ of a surface wave, which marks the end of sensor reactions to any further loading, we used the expression $\delta = [2\eta/(\omega\rho)]^{1/2}$.[21] Inserting the imaginary part of $M^{(2)}$ ($\approx\eta\omega \approx 5 \times 10^6$ N/m^2) and the density of water results in a viscous penetration depth of about 140 nm for 115 MHz and of 40 nm for 348 MHz, in good agreement with the experimental values displayed in Figure 6.

The perturbation formulas (eqs 7a,b) describing the influence of viscous loading of the device also imply the excitation of a so-called Love wave. Love waves are transverse-type surface waves guided by a film with a shear velocity lower than that of the substrate. To check this predicition, we solved the dispersion relation for Love waves[6] numerically with the parameters given in eqs 9.

On the left side of Figure 7, the numerically solved dispersion relation is shown. The step in the curve at $kh \approx 0.012$ marks the end of the acoustically thin behavior of the film; above this critical thickness, a Love wave is guided in the organic layer. This step is typical for very soft films, where the shear velocities of substrate and coating differ very much ($v_F/v_0 \approx 100$). It has nothing to do with the finite film thickness needed for the occurrence of higher Love modes![6] The so-obtained critical thickness of $h \approx 70$ nm for 115 MHz and $h \approx 25$ nm for 348 MHz is in good agreement with the experimentally determined end of the pure mass loading/acoustically thin behavior (50 and 30 nm, respectively).

A second evidence for the existence of a Love wave is obtained by calculating the normalized average acoustic energy density S

(20) Because BSA does not bind to the F_{ab} fragment, it can only be used to cover the remaining open gold surface and is *not* able to suppress cross reactions.

(21) Kanazawa, K. K.; Gordon, J. G. *Anal. Chim. Acta* **1985**, *175*, 99−105.

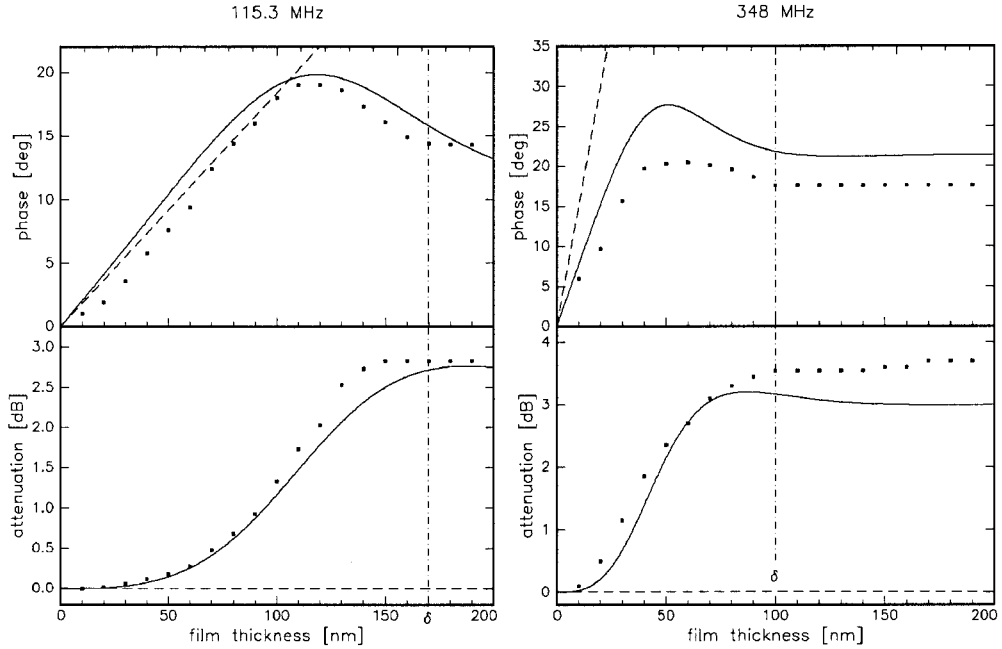

Figure 6. Response of the SAW device at 115.3 MHz (left) and 348 MHz (right) to the immobilization of 20 layers of antibodies. The solid lines are fits to eqs 7, while the dashed lines represent the effect of pure mass loading (attenuation is zero for this case). The maximum in the phase plot can be regarded as a Love wave resonance. The experimentally found viscous penetration depths of the SAW are indicated by vertical dash−dotted lines.

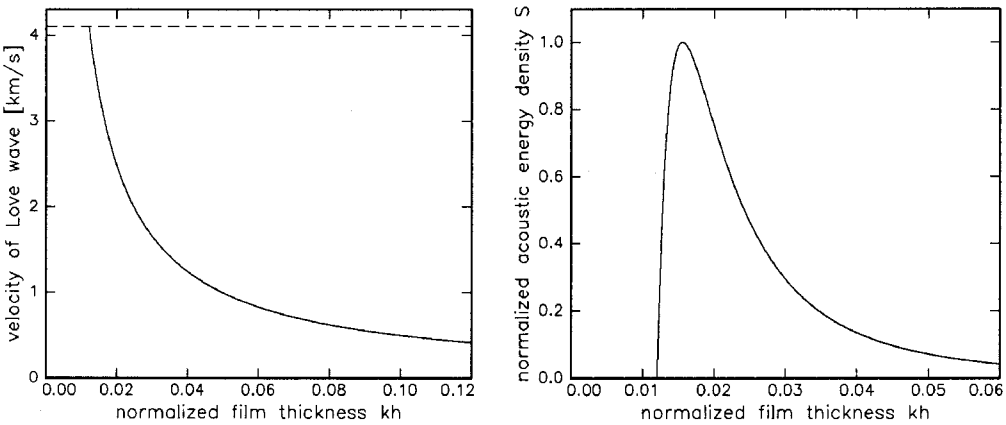

Figure 7. Love wave dispersion relation (left) and normalized average energy density versus film thickness (right) calculated with the parameters from eqs 9.

in the film, leading to the plot shown on the right side of Figure 7. The derivation of S is given in Appendix B.

It is well known that the acoustic energy density of a Love wave first grows with increasing thickness of the guiding layer but decays again with further increasing thickness. Thus, $S(h)$ should have a maximum at some thickness h_L, which can be regarded as the "resonance peak" of the Love wave. At h_L, nearly all acoustic energy is trapped in the film but not spread over too large a film volume. The peak in Figure 7 with $kh_L \approx 0.017$, and hence $h_L \approx 100$ nm and $h_L \approx 35$ nm for 115 and 348 MHz, respectively, is in good agreement with the experimentally found maxima of the phase in Figure 6.

At a first glance, our results seem to contradict the results of Rickert et al.[22] These authors have investigated very thick organic layers (about 400 nm) on a 6-MHz AT-cut quartz and found a constant sensitivity over the whole thickness range. Their results could be described with a formula similar to eq 5. But considering the perturbation formula (eq 4) and inserting elastic coefficients M, E, and densities ρ similar to those found by us shows that the argument of the hyperbolic tangent is very small for the thickness range up to 500 nm for a frequency of 6 MHz. Therefore, case 1 (ideal elastic film) is always valid in this thickness range, resulting in the observation of pure mass loading with constant sensitivity of the device, as reported in ref 22.

Finally, we would like to add two remarks. The cross-linking of the antibodies cannot be explained by pure van der Waals forces. If this was the case, an addition of BSA as second "antibody" also should lead to measurable signals $\Delta\phi$, ΔL_{dB}. After several trials, we did not observe this. Even under the assumption that, for higher-numbered layers, the film thickness increased by less than 10 nm, the curves fitted to the data had the same shape, and the fit parameters changed only slightly, staying within the same magnitude.

(22) Rickert, J.; Brecht, A.; Göpel, W. *Anal. Chem.* **1997**, *69*, 1441−1448.

CONCLUSION

From the data shown, it is evident that cross-linked antibodies build up a structure resembling a very soft polymer film, where a Love-like mode is trapped after reaching a certain thickness. The values found for the elastic coefficients compare well with those for very rubbery polymers. The sensor response is very well described by perturbation theory.

Obviously eqs 7a,b cannot fully describe the behavior of the antibody film. Not only are the fitting curves influenced by the vertical displacement component which was neglected here, but also the elastic coefficients might vary with increasing thickness. Especially within the first five antibody layers, the degree of cross-linking must change considerably, leading to an increase of the elastic coefficients. Therefore, we cannot give a perfect description of the influence of thick antibody films onto the SAW, but we can approximate it rather well and give a criterion where the "normal" perturbation formulas of Auld[4] and Kondoh and Shiokawa[9] can be used for evaluating the sensor response.

APPENDIX A

The basic equations of motion for an x_2-polarized acoustic wave propagating in the x_1 direction in an isotropic thin film are Newton's third law and Hooke's laws:

$$\sum_j \frac{\partial T_{2j}}{\partial x_j} = \rho \frac{\partial^2 u_2}{\partial t^2}$$

$$T_{21} = E^{(2)} \frac{\partial u_2}{\partial x_1}, \qquad T_{22} = 0, \qquad T_{23} = M^{(2)} \frac{\partial u_2}{\partial x_3} \tag{10}$$

where T_{ij} is the stress tensor and $E^{(j)}$, $M^{(j)}$ the usually complex elastic coefficients of the viscoelastic medium.

At a first glance, there seems to be more than two elastic constants for the isotropic medium when the restriction of pure shear displacement is dropped ($j = 1, 2, 3$), but it turns out that $E^{(j)}$ and $M^{(j)}$ can be expressed uniquely by the complex bulk and shear moduli K and G, respectively. In particular, one finds the relation $M^{(2)} = E^{(2)} = G$. With that, the derivation of eq 4 is straightforward and carried out in detail in ref 7.

The ambiguous square roots of the complex quantities $E^{(j)}$ and $M^{(j)}$ can be made single-valued by considering their physical meaning. With the condition $M', M'' \geq 0$, one chooses also $Re(M^{(j)})^{1/2}, \mathrm{Im}(M^{(j)})^{1/2} \geq 0$. Inserting reasonable values $\rho = 1000$ kg/m^3, $E^{(2)} = (1 + i) \times 10^6$ N/m^2, and $\nu_0 = 4000$ m/s shows that $[(\rho - E^{(2)})/\nu_0^2]^{1/2} \approx \rho^{1/2}$ is real-valued.

APPENDIX B

The elastic energy density, defined by

$$U = {}^1/_2 C_{ijkl} S_{ij} S_{kl} \tag{11}$$

can be evaluated for Love waves, considering that only shear displacements occur. They have the form[6]

$$u_2 = C \frac{\cos\{b_L k(h - x_3)\}}{\cos(b_L kh)}, \qquad \text{with} \qquad b_L = \sqrt{\frac{\nu^2}{\nu_F^2} - 1} \tag{12}$$

With these displacements, the strains S_{ij} in (11) can be calculated. Also, inserting $C_{2323} = G$ into (11) yields an expression for the acoustic energy density of a Love wave:

$$U = \frac{G}{2} S_{23}^2 = \frac{GC^2}{8} \frac{b_L^2 k^2 \sin^2\{b_L k(h - x_3)\}}{\cos^2(b_L kh)} \tag{13}$$

An appropriate measure for the elastic energy stored in a film of thickness h is given by averaging (13) over the entire thickness:

$$\langle U \rangle = \frac{GC^2}{8h} \int_0^h \sin^2\{b_L k(h - x_3)\}\, \mathrm{d}x_3$$

$$= \frac{GC^2}{16h} \frac{b_L k\{b_L kh - \sin(b_L kh)\cos(b_L kh)\}}{\cos^2(b_L kh)} \tag{14}$$

Normalizing this expression leads to the average energy density S, displayed in Figure 7.

ACKNOWLEDGMENT

We gratefully acknowledge financial support by the Fonds der Chemischen Industrie.

Received for review September 11, 1997. Accepted April 3, 1998.

AC971006I